JOURNAL OF Materials CHEMISTRY

Synthesis and properties of weakly coupled dendrimeric multiporphyrin light-harvesting arrays and hole-storage reservoirs†

María del Rosario Benites,[a] Thomas E. Johnson,[a]‡ Steven Weghorn,[a] Lianhe Yu,[a] Polisetti Dharma Rao,[a] James R. Diers,[b] Sung Ik Yang,[c] Christine Kirmaier,[c] David F. Bocian,*[b] Dewey Holten*[c] and Jonathan S. Lindsey*[a]

[a]*Department of Chemistry, North Carolina State University, Raleigh, North Carolina, 27695-8204, USA*
[b]*Department of Chemistry, University of California, Riverside, California, 92521-0403, USA*
[c]*Department of Chemistry, Washington University, St. Louis, Missouri, 63130-4889, USA*

Received 11th June 2001, Accepted 5th October 2001
First published as an Advance Article on the web 15th November 2001

A convergent synthesis employing porphyrin building blocks has afforded dendrimeric multiporphyrin arrays containing *n* Zn-porphyrins ($n=4$, 8, or 20) and one free base- (Fb-) porphyrin joined *via* diarylethyne linkers. Size exclusion chromatography was used extensively for purification. The arrays have sufficient solubility in toluene or other solvents for routine handling. With increasing size, the intense near-UV Soret ($S_0 \rightarrow S_2$) absorption band broadens, splits, and red shifts due to inter-porphyrin exciton coupling. In contrast, the weaker visible bands ($S_0 \rightarrow S_1$) remain essentially unchanged in position or width in proceeding from the monomer all the way to the 21-mer; however, the molecular extinction coefficients of the visible bands scale with the number of porphyrins. Similarly, the one-electron oxidation potentials of the porphyrins are virtually unchanged as the arrays get larger. These results are indicative of relatively weak (but significant) electronic coupling between ground states and between the photophysically relevant lowest-excited-singlet states of the diarylethyne-linked porphyrins; thus, the characteristic properties of the individual units are retained as the architectures increase in complexity. Efficient excited-singlet-state energy transfer occurs among the Zn-porphyrins and ultimately to the sole Fb-porphyrin in each of the arrays, with the overall arrival time of energy at the trapping site increasing modestly with the number of Zn-porphyrins = 1 (45 ps), 2 (90 ps), 8 (105 ps), and 20 (220 ps). The overall energy-transfer efficiencies are 98%, 96%, 96%, and 92% in the same series. The ground-state hole-storage properties of the 21-mer ($Zn_{20}Fb$) were examined. Bulk electrolysis indicates that 21 (or more) electrons can be removed from this array (*e.g.*, one hole resides on each porphyrin) to yield a stable "super-charged" π-cation radical. Taken together, these results indicate that the convergent building-block synthesis approach affords dendrimeric multiporphyrin arrays with favorable properties for light-harvesting and hole storage.

Introduction

As part of a program in artificial photosynthesis, we have been working on the design, synthesis, and characterization of multiporphyrin light-harvesting arrays.[1] Synthetic multiporphyrin arrays are useful models of natural photosynthetic antennas and also provide the basis for a variety of molecular photonic devices, including sensors, nanoscale optical sources, and solar collectors. An effective light-harvesting array absorbs intensely and transfers the resulting electronic excited-state energy to one site with high efficiency. Accordingly, the strong light-absorbing properties of porphyrins make these macrocycles ideal for light-harvesting applications.[2] Multiporphyrin arrays can also function as nanoscale hole/electron storage reservoirs because porphyrins form relatively stable π-cation radicals. Thus, a multiporphyrin construct affords the possibility of storing large numbers of electron equivalents.[3,4]

Two basic types of approaches have been taken in the design of multi-chromophoric arrays for light-harvesting applications. Both approaches have favorable characteristics depending on the desired properties, design constraints, and assembly strategies. One approach employs linkers that give very strong electronic interactions between the units.[5–11] In the strong coupling limit, such constructs typically exhibit supermolecular properties in that energy/electron delocalization involves wavefunctions that extend over a large number of chromophores. Consequently, such arrays have many characteristics that are much different from those of the isolated pigments, and that can change substantially with the size and architecture of the assembly. The second approach employs linkers that give rather modest couplings between pigments: such couplings are sufficiently weak so that key properties (*e.g.*, ground-state redox potentials, photophysical characteristics of the lowest excited singlet state) designed into the individual pigments are essentially retained in the arrays, yet are of sufficient magnitude to support ultrafast excited-state energy transfer and facile

†Electronic supplementary information (ESI) available: a description of multiphoton effects at high excitation intensities; the complete Experimental section including descriptions of the syntheses of the arrays; SEC data, ^{1}H NMR spectra, and mass spectra for all new porphyrins and multiporphyrin arrays; a description of exploratory studies in the purification of $Zn_{20}Fb$; data from a comparative study of analytical SEC conditions; representative mass spectral data under different conditions; and representative absorption and fluorescence spectra of the arrays. See http://www.rsc.org/suppdata/jm/b1/b105108n/

‡Contribution from the Department of Chemistry, Carnegie Mellon University. Current address: Department of Chemistry, University of Georgia, Athens, GA 30602, USA.

DOI: 10.1039/b105108n

ground-state hole/electron hopping. We have chosen this second strategy and have found that the diarylethyne linker affords the desired inter-pigment couplings, molecular properties, and wide versatility in a molecular building-block approach.[2–4,12–23]

Several distinct routes have been reported for synthesizing multiporphyrin arrays with potential light-harvesting properties. *Self-assembly* routes have afforded windowpane arrays of Pd-coordinated pyridyl-substituted porphyrins,[24] indefinite aggregates of Zn-chlorins bearing hydroxy and keto groups,[25] discrete aggregates of pyridyl-coordinated Zn-porphyrins,[26] and other diverse architectures.[27] *Polymerization* approaches have yielded backbone polymeric arrays of up to 128 porphyrins with direct *meso–meso* linkages,[9] or shorter polymers with oligo(phenylenevinylene),[28] phenylethyne,[29] or butadiyne linkers.[30] *Stepwise synthesis* procedures have afforded the majority of synthetic light-harvesting arrays. The chemistries employed have included (1) Wittig reactions affording stilbene linkers;[31] (2) Sonogashira reactions affording diphenylethyne,[2,12–23] oligophenylethyne,[32] or diethynylethene linkers;[33] (3) Glaser reactions affording diphenylbutadiyne linkers;[23,34] (4) Heck reactions yielding ethene linkers;[35] (5) condensation reactions affording phenylene linkers;[36,37] (6) alkylation reactions affording benzoxyphenyl linkers,[38] polyalkoxy linkers[39] or 1,3,5-triazine units joining aniline groups;[40] (7) amide forming reactions,[41,42] and (8) a sequence of complementary chemistries including the Sonogashira reaction affording diphenylethyne and other linkers.[17,43,44] It is noteworthy that some routes have led to porphyrin dendrimers. In particular, dendrimers have been prepared that are composed of one porphyrin at the core;[45] 16,[41] 32,[42] or 64,[41] porphyrins at the periphery; or up to 21 porphyrins in the framework of the dendrimer.[37]

We have employed the Sonogashira reaction[46] in a building block approach for the modular construction of covalently linked multiporphyrin arrays.[2,23] This modular route takes advantage of the availability of porphyrin building blocks with control over the pattern of the substituents at the four *meso*-positions. The typical substituents are aryl rings that bear solubilizing groups (*e.g.*, mesityl) and/or synthetic handles (*e.g.*, iodo and ethynyl groups) for further elaboration. The porphyrins are used as the free base (Fb) or metal chelate. The Pd-coupling reactions of iodophenyl and ethynylphenyl porphyrin building blocks yield diarylethyne linkages and are performed under mild, non-acidic, non-metalating conditions, which preserve the metalation state of the porphyrin building blocks.[47,48] The diarylethyne linker undergoes a modest degree of bending[49] and enables free rotation (about the cylindrically symmetric ethyne unit), thereby affording a relatively fixed distance of separation and access to all dihedral angles of adjacent linked porphyrins.[50] We have employed this synthetic approach to construct arrays consisting of porphyrins or porphyrins plus accessory pigments in linear,[2,13,21] T-shaped,[51] star-shaped,[12,19] cyclic,[16] or square[15] architectures. The constructs include light-harvesting arrays, optoelectronic gates, and a variety of dyads and triads to probe the mechanisms of excited-state energy transfer and ground-state hole/electron hopping between porphyrins and between porphyrins and accessory chromophores. Each of our diarylethyne-linked arrays prepared and studied to date has been comprised of six or fewer porphyrins. A selection of such arrays includes dimers (ZnFbU,[23] ZnFbP,[2] Zn_2 [23]), molecular squares (*cyclo*-Zn_2Fb_2U, *cyclo*-Zn_4U),[15] trimers (Zn_3, ZnZnFb),[2] and star-shaped pentamers (Zn_4FbU, Zn_5U)[12,19] as shown in Charts 1 and 2;[52] the properties of these arrays provide the benchmarks for understanding the properties of the new arrays described herein.

In this paper, we have extended the building block approach to the synthesis of dendrimeric multiporphyrin arrays containing up to five, eight, nine, or 21 porphyrins. The arrays contain Zn-porphyrins and one (or no) Fb-porphyrin and are joined *via* diarylethyne linkers. Issues related to synthesis include the size of the array that can be constructed, the solubility of the larger arrays, and the use of size exclusion chromatography (SEC) as a means of purification. The arrays have been characterized by static and time-resolved optical spectroscopy to investigate their light-harvesting and energy-funneling characteristics, and electrochemistry to probe their hole-storage capabilities.

Results and discussion

1. Molecular design

Our objective was to prepare a family of dendrimeric arrays in which a single Fb-porphyrin resides at the core of the assembly and a variable number of Zn-porphyrins project outward from the core. The overall architecture depends on (1) the design of the Fb-porphyrin building block (which influences the shape of the array *via* the directions in which the Zn-porphyrin-containing antenna unit is attached) and (2) the number of generations of Zn-porphyrins (which influences the size of the array). The diarylethyne linker that joins the porphyrins is semi-rigid[49] and allows significant electronic communication between the porphyrins.[3,4,20,53] The non-linking *meso*-positions are substituted with mesityl groups to engender solubility in organic solvents.

2. Synthesis

Strategy. Porphyrin-based dendrimeric arrays bearing diphenylethyne linkers can be prepared in either a convergent or divergent manner. In a convergent route, the periphery of the array is constructed first and the synthesis proceeds inward toward the core of the dendrimer. For a porphyrin with at most four connections, this approach affords no more than four sites of coupling per transformation. In a divergent route, the synthesis begins at the core of the array and works outward. In the synthesis of a nonamer, for example, coupling at six sites would be required in the final step, which could hamper purification of the desired array. The convergent route is advantageous in that fewer side products are produced as the result of incomplete coupling. The syntheses of the arrays described herein were carried out in a convergent manner. The synthesis of the arrays was performed in the period of 1993–1998 using the methods available at the time.

Porphyrin building blocks. The *meso*-tetraarylporphyrins bearing one, two or four functional groups (iodo and/or trimethylsilyl- (TMS)-ethyne groups) served as the basic building blocks for the synthesis of the multiporphyrin arrays (Chart 3). The porphyrin building blocks Zn-H (also termed Zn-U′),[47] I-Zn-TMS,[2] I-Fb-I,[54] I_3-Fb-TMS,[23] I_4-Fb,[23] and I-Fb[48] were obtained as previously reported. An improved procedure for the purification of I_3-Fb-TMS afforded the Fb-porphyrin in 18% yield, compared to 9.8% yield obtained previously.[23]

Preparation of arrays. *(a) Tetramers.* The reaction of I_3-Fb-TMS and Zn-H was performed using standard Pd-mediated coupling conditions[47] (Scheme 1). These conditions include $\sim$2.5 mM concentrations of reactants with $Pd_2(dba)_3$ and $AsPh_3$ in toluene/triethylamine at 35 °C under Ar in the dark. These conditions avoid the use of copper reagents, afford coupling in dilute solution, and do not alter the metalation states of the porphyrin building blocks. The reaction was monitored by analytical SEC.[22,47] After 20 h, the analytical SEC showed four peaks consisting of the following materials (absorption data uncorrected for extinction coefficients): higher molecular weight material (HMWM, 5%), desired tetramer and other unidentified products (75%), dimeric product (3%), and unidentified monomeric porphyrins (17%). Purification by

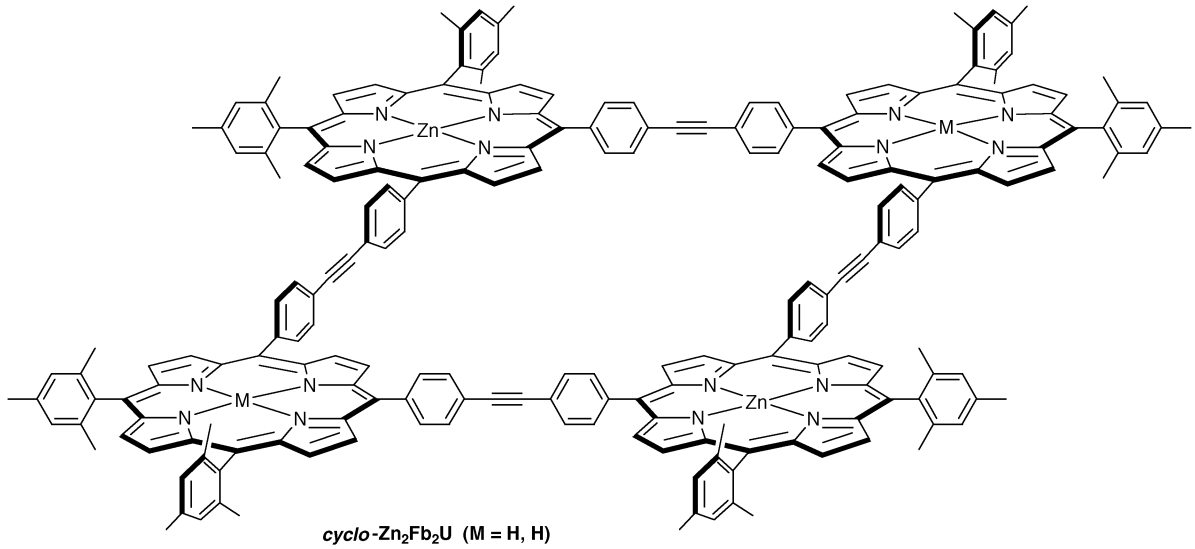

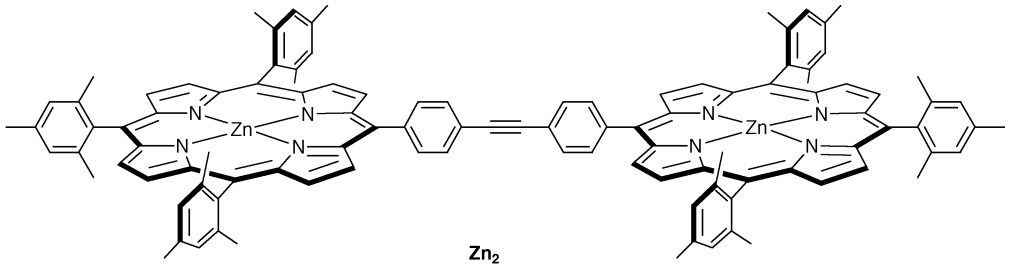

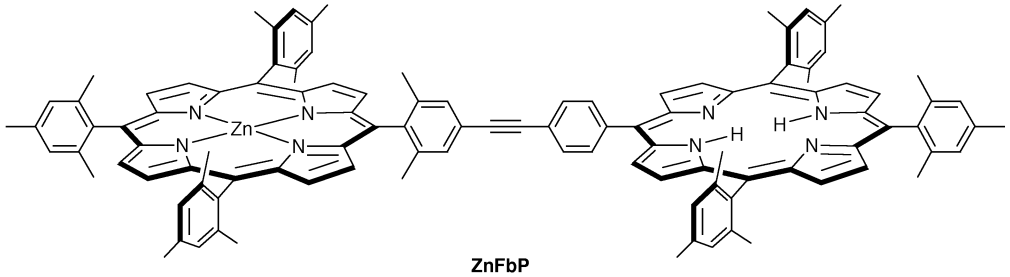

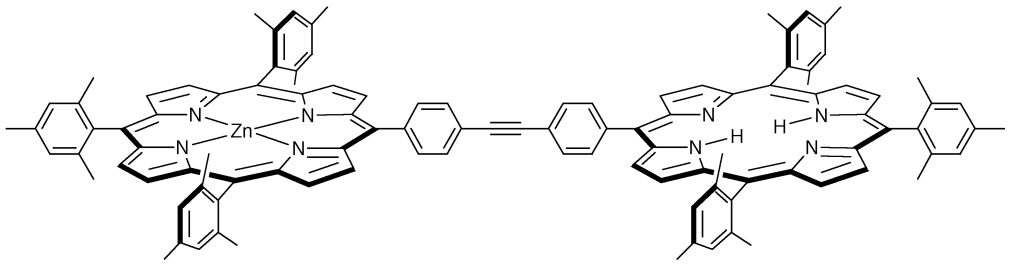

Chart 1 Representative arrays prepared previously.[50,52]

chromatography (silica and preparative SEC) afforded the Zn_3Fb-TMS tetramer in 61% isolated yield. Metalation of Zn_3Fb-TMS with $Zn(OAc)_2{\cdot}2H_2O$ afforded the all-Zn-tetramer Zn_4-TMS in 92% yield. Treatment of Zn_4-TMS with Bu_4NF in THF for 1 h at room temperature gave the monoethyne-substituted tetramer Zn_4-H (94%). The arrays Zn_3Fb-TMS, Zn_4-TMS and Zn_4-H provided satisfactory absorption, ^1H NMR, and laser-desorption mass spectrometry (LD-MS) data. The constitution of Zn_4-H was further confirmed by high-resolution mass spectrometry (HRMS) analysis. The tetramer Zn_4-H was employed in a molecular dynamics study using ^1H NMR spectroscopy to assess the motional freedom of the linker (rotation and bending),[49] and as the antenna component of integrated antenna-reaction center complexes.[18] The tetramer Zn_4-H also was converted to a diphenylbutadiyne-linked Zn_8 octamer *via* Glaser oxidative homocoupling (Electronic Supplementary Information†). The Zn_8 octamer lacks a Fb-porphyrin to serve as a low-energy trapping site for light-harvesting applications.

(b) Asymmetric pentamer Zn_4Fb. A star-shaped pentamer was prepared which differs from the star-shaped pentamers

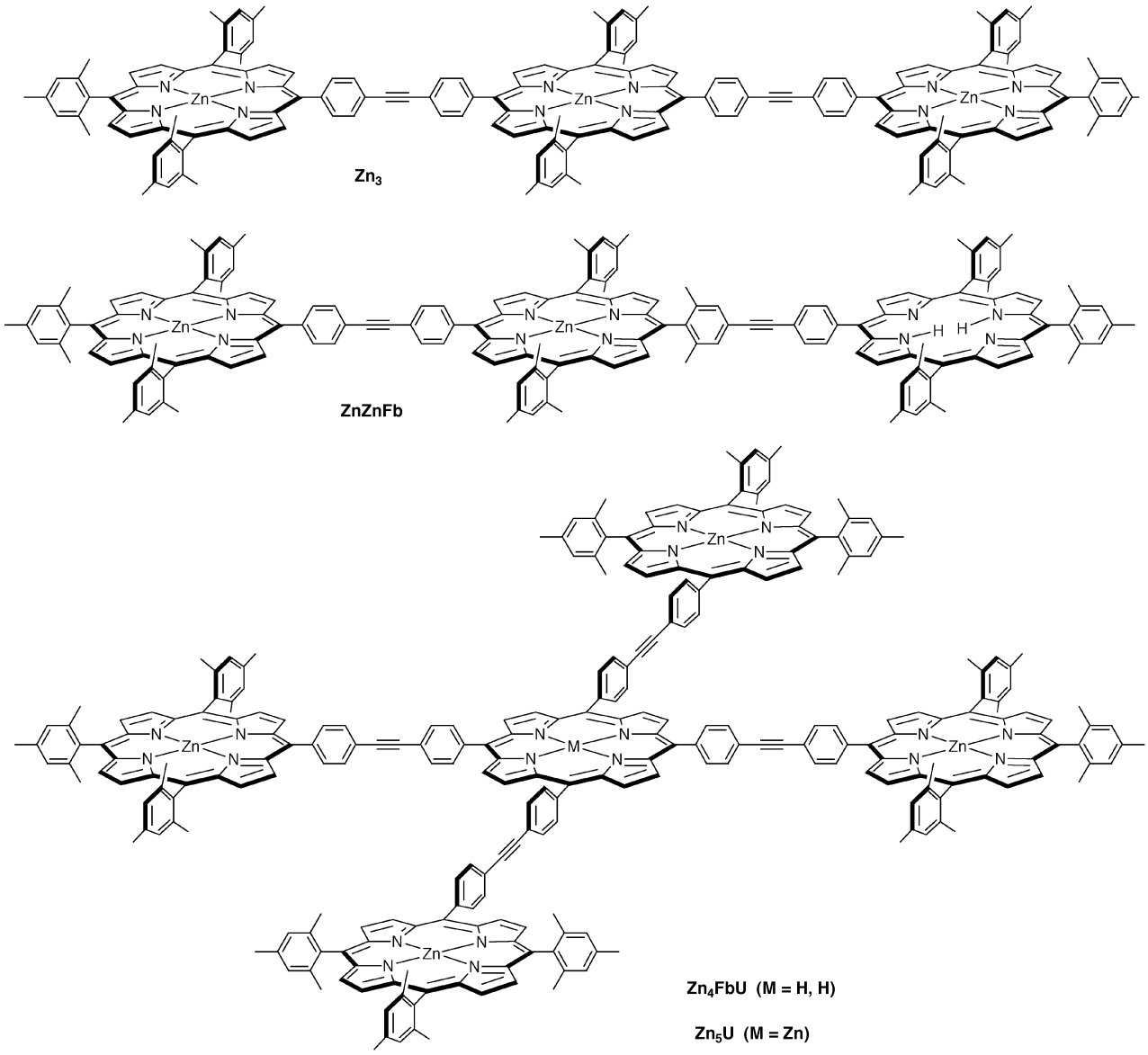

Chart 2 Representative arrays prepared previously.[50,52]

that we have prepared previously. The latter have 4-fold symmetry with a core Fb-porphyrin and four identical metalloporphyrins at the periphery of the array. In contrast, the asymmetric Zn_4Fb pentamer incorporates the Fb-porphyrin at the periphery of the array (Scheme 2). This light-harvesting array was prepared in 81% yield by the Pd-mediated coupling of the mono-ethynyl tetramer Zn_4-H with a mono-iodo Fb-porphyrin (I-Fb). Analysis by absorption spectroscopy, ^{1}H NMR spectroscopy, and LD-MS afforded satisfactory data.

(c) Nonamer Zn_8Fb. Tetramer Zn_4-H also served as a monoethynyl building block in the convergent synthesis of a nonameric array. Thus, coupling of the diiodo Fb-porphyrin I-Fb-I and Zn_4-H for 19 h afforded nonamer Zn_8Fb (Scheme 3). In this array, the core porphyrin is surrounded by two tetrameric porphyrin units *trans* to each other. Analytical SEC of the reaction mixture showed 90% conversion of the starting porphyrins to the nonamer, as well as some HMWM, pentameric and tetrameric species (Fig. 1). After preliminary purification by silica chromatography, the mixture was subjected to preparative SEC. The HMWM and the nonamer overlapped substantially on the gravity-flow SEC columns. The use of THF instead of toluene as eluent or a decrease in the flow rate did not provide improved separation. Silica chromatography [CH_2Cl_2/hexanes (2 : 1)] helped remove the HMWM to some extent (leading band on the column) but with significant loss of material ($\sim$20%). In contrast, material losses were negligible with SEC. Accordingly, repetitive SEC was used in lieu of silica chromatography. Thus, a series of 7–9 SEC columns (for 20 mg of material) became necessary to obtain pure Zn_8Fb as a red-purple solid (3.6 mg, 20% isolated yield). The purified sample of Zn_8Fb gave a sharp peak in analytical SEC (Fig. 1C) and provided satisfactory absorption, ^{1}H NMR and LD-MS data. Three side products were also isolated from SEC and analyzed by LD-MS: the intermediate pentamer Zn_4Fb-I ($<$1%), and two phenyl-derivatized pentameric and tetrameric species of unidentified structure, Zn_4Fb-Ph ($<$1%) and Zn_4-Ph (2%). Metalation of Zn_8Fb using $Zn(OAc)_2{\cdot}2H_2O$ afforded the all-Zn-nonamer Zn_9.

(d) Pentamer Zn_5-H. The synthesis of larger arrays was initiated by the preparation of a mono-ethynyl pentameric array. Thus, tetramer Zn_4-H and I-Zn-TMS were subjected to the standard Pd-mediated coupling conditions (Scheme 4). After 4 h, the analytical SEC showed HMWM (9%), the desired pentamer along with a tetramer (80%), and monomeric species (10%) (data uncorrected for extinction coefficients). A combination of silica chromatography and SEC afforded pure

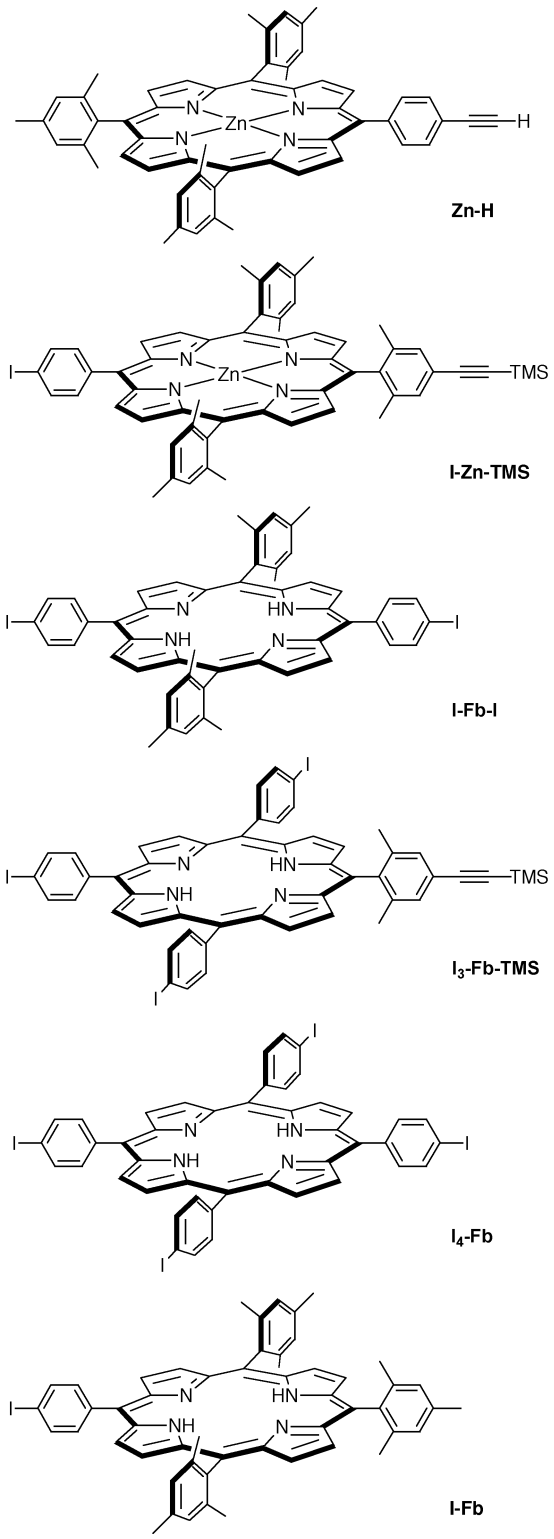

Chart 3 Monomeric porphyrin building blocks.

Zn_5-TMS in 66% yield. Analytical SEC of the purified sample showed a single sharp peak. The absorption, ^{1}H NMR, LD-MS and HRMS data of Zn_5-TMS were satisfactory. A putative phenyl-capped Zn_4-porphyrin (Zn_4-Ph, 10%) and octamer Zn_8 (5%, *vide infra*) were also obtained as side products. Removal of the TMS group from Zn_5-TMS with Bu_4NF afforded Zn_5-H in 95% yield.

(e) 21-mer Zn_{20}Fb. A convergent synthesis of Zn_{20}Fb was performed by reaction of the Fb-porphyrin I_4-Fb with four molar equivalents of pentamer Zn_5-H under the standard Pd-coupling conditions (Scheme 5). After 3.5 h, analytical SEC indicated very slow reaction. Therefore, additional amounts of $Pd_2(dba)_3$ and $AsPh_3$ were added. After 22 h, analytical SEC indicated incomplete consumption of monomer and pentamer but LD-MS analysis showed the formation of Zn_{20}Fb (*m/z* obsd 16691.2, calcd 16693.0). Several products co-eluted on analytical SEC [HMWM, desired 21-mer, and other reaction products (16-mer and 11-mer resulting from incomplete coupling)] (Fig. 2). A further increase in the reaction time or the amount of Pd catalyst did not affect the yield of the array. This trend is in line with the multiple coupling reactions employed in the synthesis of Zn_3Fb-TMS or Zn_8Fb.

The 21-mer could not be purified by the standard methods of column chromatography. After investigating a variety of separation methods (see Electronic Supplementary Information†), we turned to the use of semi-preparative SEC–HPLC columns. The optimum set of conditions for separation of the 21-mer on analytical SEC–HPLC was one 10^3 Å column or two 10^3 Å columns in series, a flow rate of 0.8 mL min^{-1}, and THF as the mobile phase, but only 50–100 μg could be partially purified in each run. The use of a preparative HPLC–SEC (10^3 Å) column allowed larger sample injections ($\sim$2 mg). A flow rate of 3.0 mL min^{-1} offered a good compromise between peak separation and run time [retention time (Zn_{20}Fb) = 22.1 min], affording Zn_{20}Fb as a broad peak with some tailing of porphyrins for over 15 min. Fractions (0.5–1.0 mL) were cut and impure fractions were rechromatographed. A total of 5–7 HPLC–SEC separations (for 5–8 mg of material) were carried out to yield pure Zn_{20}Fb (1.9 mg, 19%). Analytical SEC of the purified sample gave a single sharp peak (Fig. 2D). Satisfactory absorption and MALDI-MS data were obtained but a well resolved ^{1}H NMR spectrum was not obtained. Metalation of Zn_{20}Fb with $Zn(OAc)_2 \cdot 2H_2O$ gave the all-zinc 21-mer Zn_{21}.

In summary, the convergent synthetic approach affords diarylethyne-linked arrays in sufficient quantities for spectroscopic studies. The yields and ease of purification were satisfactory for the tetramer and pentamers (Zn_3Fb-TMS, 61%; Zn_5-TMS, 66%; asymmetric Zn_4Fb, 81% yield) but the larger arrays were obtained in lower yield following extensive chromatography (Zn_8Fb, 20%; Zn_{20}Fb, 19% yield). We are currently working to develop refined approaches to obtain multiporphyrin arrays. It is noteworthy that a dendrimeric array similar in architecture to that of Zn_{20}Fb, but incorporating 20 nickel porphyrins and one Fb-porphyrins with *p*-phenylene linkers, has been prepared *via* successive porphyrin-forming reactions.[37]

3. Use of SEC for the purification of multiporphyrin arrays

The successful purification of the larger multiporphyrin arrays proved challenging. We have employed SEC to purify and analyze multi-porphyrin arrays previously.[2,22,23,47] However, with arrays comprised of more than five porphyrins, separation by SEC using the resins employed herein became extremely difficult. Arrays containing up to nine porphyrins were successfully purified by a combination of adsorption chromatography and repetitive SEC.

The availability of a family of arrays of increasing size but otherwise similar architectures prompted the comparison of the chromatographic mobilities with analytical SEC columns of different pore size. The elution patterns of a family of seven arrays containing 1–5, 9 and 21 porphyrins on four different analytical SEC columns (100, 500, 10^3, 10^4 Å) are shown in Fig. 3. All arrays elute according to molecular size. The 500 Å or 10^3 Å column provides superior separation for all members of this set of arrays. The metalation state does not influence the retention time of the porphyrin array in SEC, as Fb-porphyrins and metalloporphyrins with the same structure eluted with nearly identical retention times.

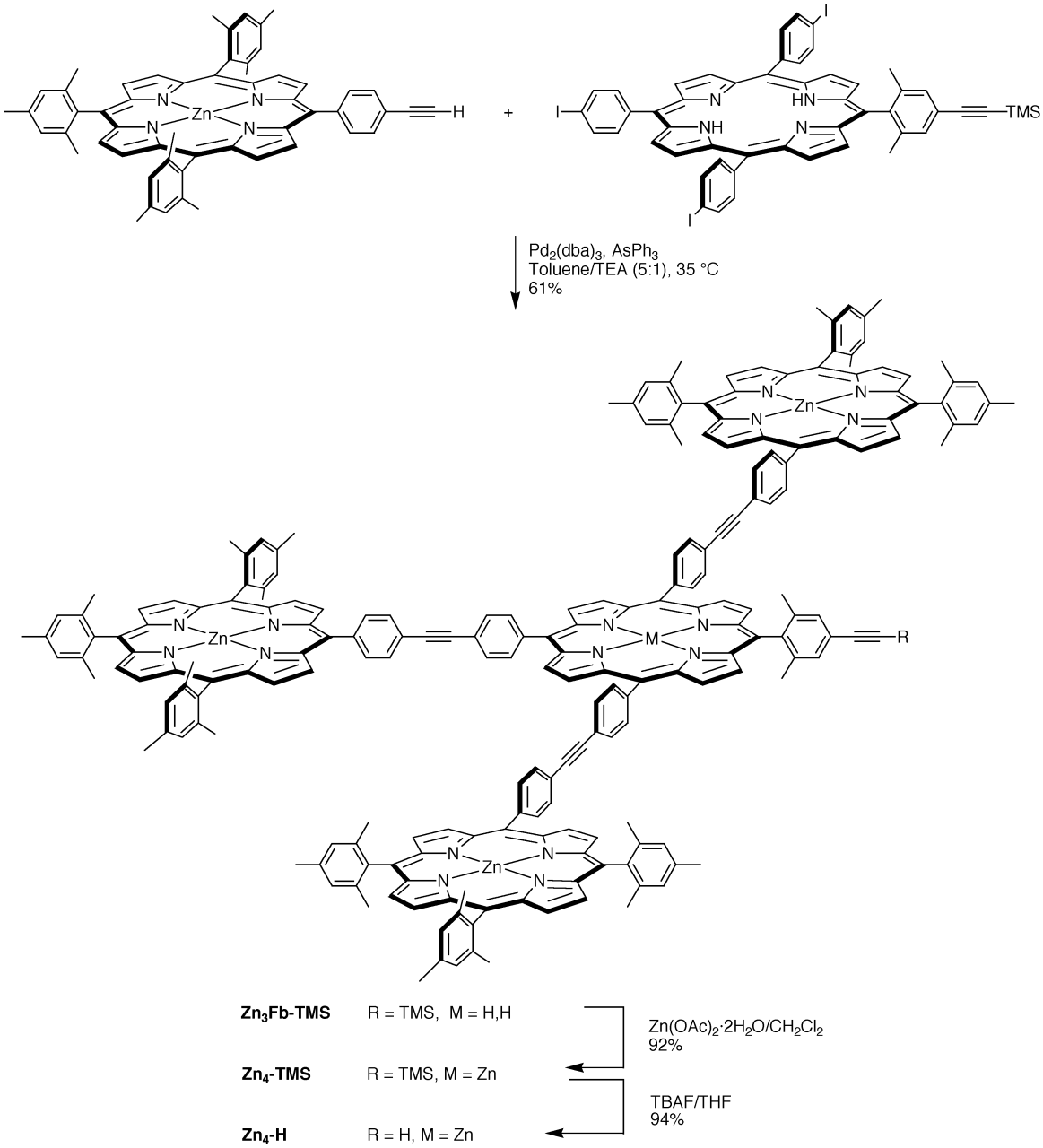

Scheme 1 Synthesis of tetrameric arrays.[50]

4. LD-MS analysis of multiporphyrin arrays

In a prior study, we investigated the application of LD-MS and matrix-assisted laser desorption ionization mass spectrometry (MALDI-MS) to a collection of porphyrin monomers[55] and a series of multiporphyrin arrays extending to a nonamer.[56] Examination of the porphyrin monomers showed that the ionization process afforded intact molecule ion peaks (*i.e.*, the cation radical rather than the protonated species). While porphyrin monomers and small arrays typically afford high quality spectra without a matrix (*i.e.*, LD-MS), the study of the multiporphyrin arrays showed that the use of a matrix afforded higher quality spectra as the arrays increased in size (>5 porphyrins). Regardless of substrate, the soft ionization method of LD-MS or MALDI-MS preserves the metalation state of porphyrin arrays and allows successful analysis of arrays containing both Fb- and metallo-porphyrins.

For the characterizations performed herein, intact, singly ionized molecules were observed for each of the arrays. Mass measurements agreed with the expected theoretical values within 0.3% accuracy. The matrices 4-hydroxy-α-cyano-cinnamic acid (4-HCCA) and ferulic acid (*trans*-4-hydroxy-3-methoxycinnamic acid), in saturated solutions of $CHCl_3$ or toluene, were investigated for the analysis of the arrays comprised of 9 or 21 porphyrins. The best results (based on the signal intensity of the molecule ion peak under the same experimental conditions) were obtained using ferulic acid in toluene as matrix, followed closely by 4-HCAA in toluene. The spectrum with ferulic acid afforded a stronger molecule ion peak and less fragmentation (see Electronic Supplementary Information†).

All arrays containing four, five or nine porphyrins exhibited a similar fragmentation pattern with peaks separated by approximately 728 and 904 Da from the parent ion, corresponding to the loss of a peripheral trimesityl Zn-porphyrin and a trimesityl Zn-porphyrin containing a diphenylethyne linker, respectively, from the array. Some information was also obtained concerning the composition of the HMWM. The LD-MS data indicate that SEC fractions containing HMWM consisted of mixtures of materials in which one to 8–9

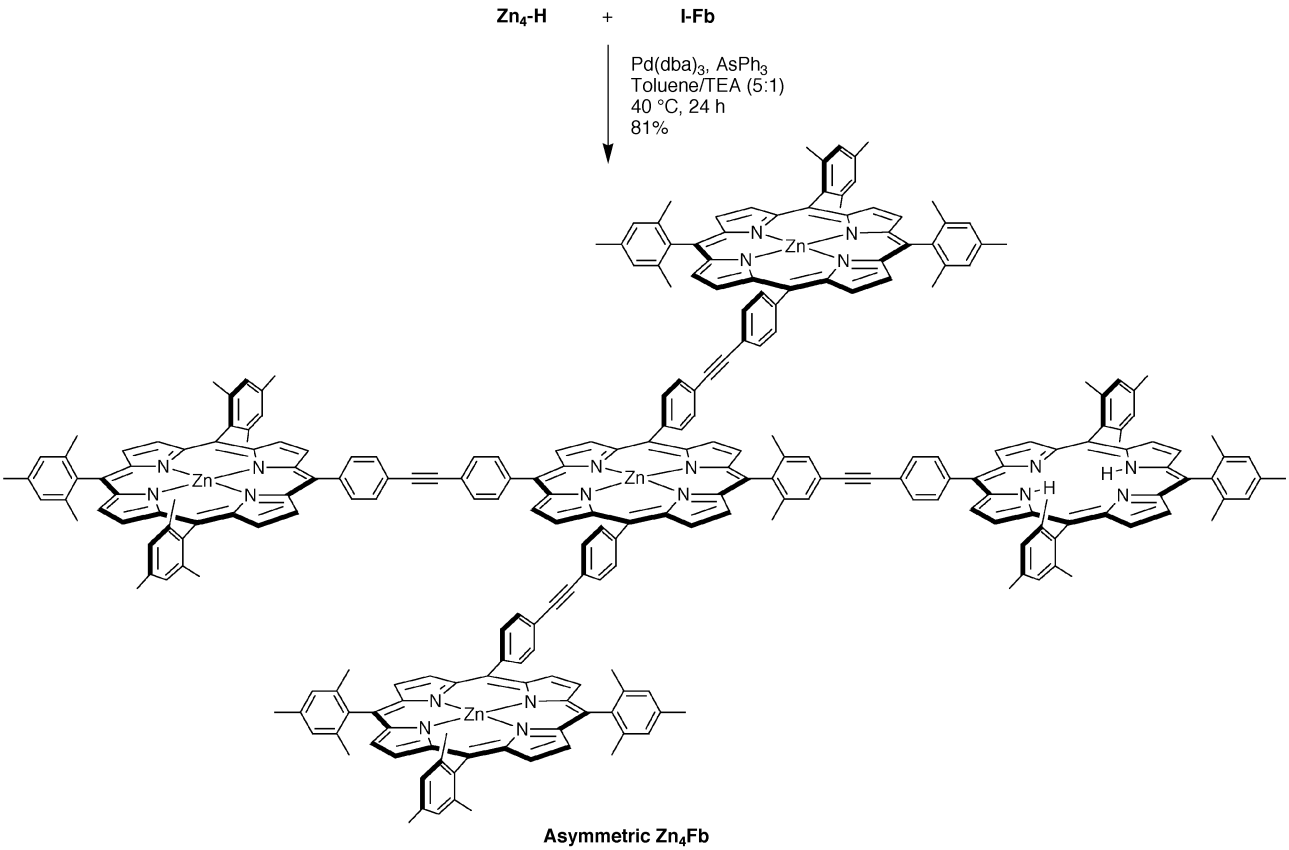

Scheme 2 Synthesis of the asymmetric Zn_4Fb pentamer.[50]

additional porphyrins are attached to a structure of mass corresponding to that of the desired array.

5. Solubility

All multiporphyrin arrays, with the exception of Zn_4-H and Zn_5-H, exhibit high solubility in toluene, THF, $CHCl_3$ and CH_2Cl_2. The mesityl groups at the periphery of the arrays provide sufficient steric encumbrance of the porphyrin macrocycles to suppress cofacial aggregation. Moreover, the motion afforded by the flexibility (rotational freedom and bending)[49] of the diphenylethyne linker permits good solubility relative to arrays containing more rigid linkages, such as molecular square arrays *cyclo*-Zn_2Fb_2U and *cyclo*-Zn_4U.[15] In contrast to their trimethylsilyl protected counterparts, Zn_4-H and Zn_5-H are only slightly soluble in halogenated solvents. Zn_4-H shows relatively high solubility in toluene and THF, while Zn_5-H is freely soluble only in THF. As one operational measure of solubility, we were able to obtain ^{1}H NMR spectra of a number of the arrays at typical concentrations ($\sim$1 mM) without noticeable aggregation.

6. Photophysical properties

Static absorption spectroscopy. The near-UV/Vis absorption spectra of a series of all-Zn-porphyrin arrays ranging from monomer to 21-mer are shown in Fig. 4. The visible-region features between 500 and 700 nm are shown on an expanded absorbance scale in Fig. 5. Peak wavelengths and extinction coefficients are given in Table 1. As a reference, the spectrum of the ZnTPP (TPP = tetraphenylporphyrin) monomer contains the intense near-UV Soret B(0,0) band at 423 nm and the much weaker B(1,0) vibronic feature at $\sim$400 nm; these Soret features correspond to transitions from the ground state to the second excited singlet state ($S_0 \rightarrow S_2$). The ZnTPP spectrum also shows the weaker visible bands corresponding to the transitions from the ground state to the lowest excited singlet state ($S_0 \rightarrow S_1$); these features are the Q(0,0) band at 588 nm and the Q(1,0) vibronic band at 549 nm, with the latter being more intense than the former due to vibronic borrowing from the intense Soret transition.[57]

As the arrays progressively increase in size, some characteristics of the absorption spectra change appreciably while others do not. In the former category are the characteristics of the Soret ($S_0 \rightarrow S_2$) absorption. Fig. 4 shows that the Soret band red shifts and splits (6–8 nm from Zn_3 to Zn_{21}) with increasing number of porphyrins in the array. These effects are well understood in terms of the pronounced exciton interactions between the large transition dipoles (reflected in $\varepsilon \sim 5 \times 10^5$ M^{-1} cm^{-1}) of the Soret transitions of adjacent porphyrins, as we have described for star-shaped pentameric and smaller multiporphyrin arrays.[19,20]

On the other hand, the positions and widths of the Q bands (500–600 nm) remain virtually unchanged with increasing array size, except for a small red shift in the features (Fig. 5). The small spectral shift with increasing array size can be understood in terms of factors that include (1) the environmental effect of each Zn-porphyrin being surrounded by more porphyrins and less solvent than in smaller arrays, and (2) effects of relatively small interactions between the weak Q-transitions of adjacent porphyrins (for which the exciton splittings are expected to be less than the energy-widths of the bands[58]). It is also noteworthy that the molar decadic extinction coefficients (ε) of the Q bands scale approximately linearly with the number of Zn-porphyrins in an array. For example, for the Q(1,0) transition, Zn_5-TMS exhibits $\varepsilon = 110\,000$ M^{-1} cm^{-1} which is 5 times that of ZnTPP ($\varepsilon = 22\,000$ M^{-1} cm^{-1}) (Table 1).

The observations on the Q bands reflect the fact that the linker-mediated inter-porphyrin interactions in the photophysically most relevant excited electronic state (S_1) are relatively small. Furthermore, the results obtained here show that this is true even when considering the composite interactions that exist in an array with 21 porphyrins. The consequences include the following: (1) the inherent excited-state decay properties of

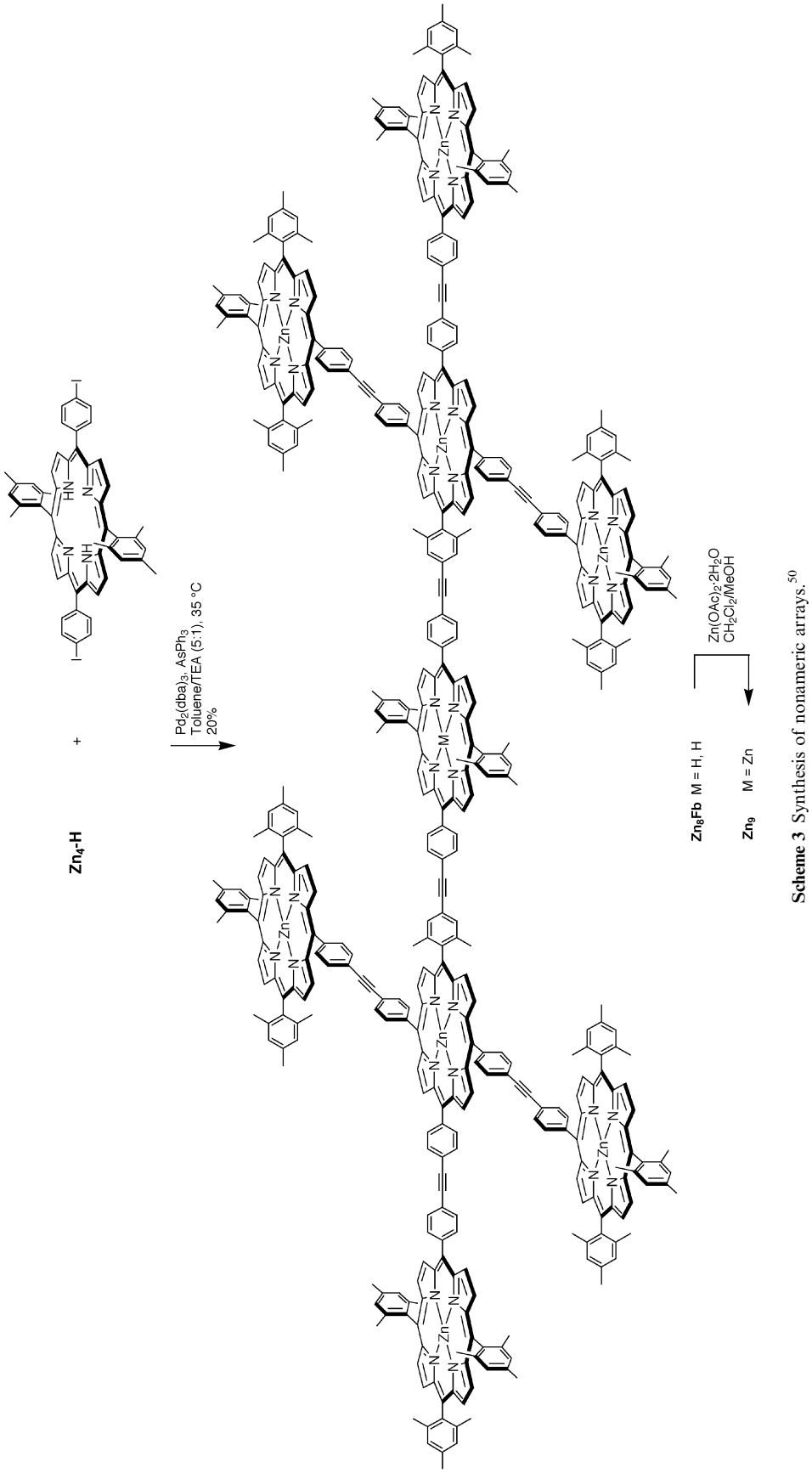

Scheme 3 Synthesis of nonameric arrays.[50]

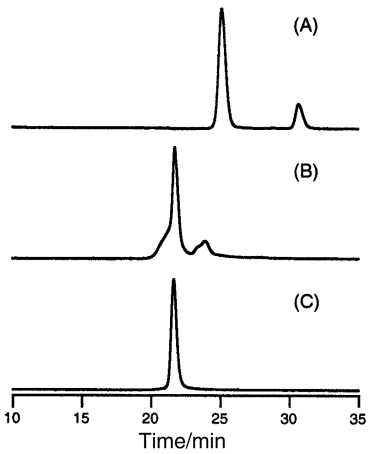

Fig. 1 SEC traces for the synthesis of Zn_8Fb using 1000, 500, and 100 Å columns in series. (A) Reaction mixture before the addition of Pd-catalyst. (B) Reaction mixture after 19 h. (C) Purified Zn_8Fb.

the isolated porphyrin (microscopic rate constants for fluorescence, internal conversion, intersystem crossing) are retained for each porphyrin in the large arrays, and can be used as a benchmark for assessing additional processes that may occur in the arrays, such as excited-state energy transfer; (2) properties designed into the individual chromophores or smaller units will be retained (and need not be re-evaluated) as the architectures become increasingly larger and complex. We have previously noted these findings and expectations regarding the S_1 excited state from detailed photophysical studies on smaller arrays,[15,16,19,20] and find them to be manifest in the very large assemblies prepared and studied here. (Analogous conclusions regarding weak, but significant, inter-porphyrin electronic communication in the ground electronic state are drawn from the similarity in the redox properties of arrays with increasing size, as is described below.) It is also noteworthy that the increasing extinction coefficients of the Q-bands with increasing number of porphyrins in the array (Figures 4 and 5; Table 1) afford larger optical cross sections that enhance the light-harvesting function of the extended architectures relative to the smaller architectures.

The absorption spectra of the arrays containing a central Fb-porphyrin and either eight Zn-porphyrins (Zn_8Fb) or 20 Zn-porphyrins ($Zn_{20}Fb$) are shown in Fig. 6. These spectra are dominated by the spectral characteristics of the multiple Zn-porphyrins and are thus very similar to those of the all-Zn-porphyrin analogs Zn_9 and Zn_{21} (Figures 4 and 5). The Soret band of the Fb-porphyrin is buried under the intense Soret absorption of the Zn-porphyrins; similarly, the Fb-porphyrin $Q_Y(0,0)$ and $Q_X(1,0)$ bands at $\sim$550 and $\sim$590 nm are buried under the Zn-porphyrin Q(1,0) and Q(0,0) bands at these wavelengths. Close inspection of the visible-region spectra of Zn_8Fb and $Zn_{20}Fb$ shows the presence (with the appropriate relative intensity) of the Fb-porphyrin $Q_Y(1,0)$ band at 515 nm, and particularly the $Q_X(0,0)$ band at $\sim$650 nm that is well removed from any Zn-porphyrin features (see Electronic Supplementary Information†).

Static emission spectroscopy. The room temperature steady-state fluorescence spectra of the all-Zn-porphyrins, including

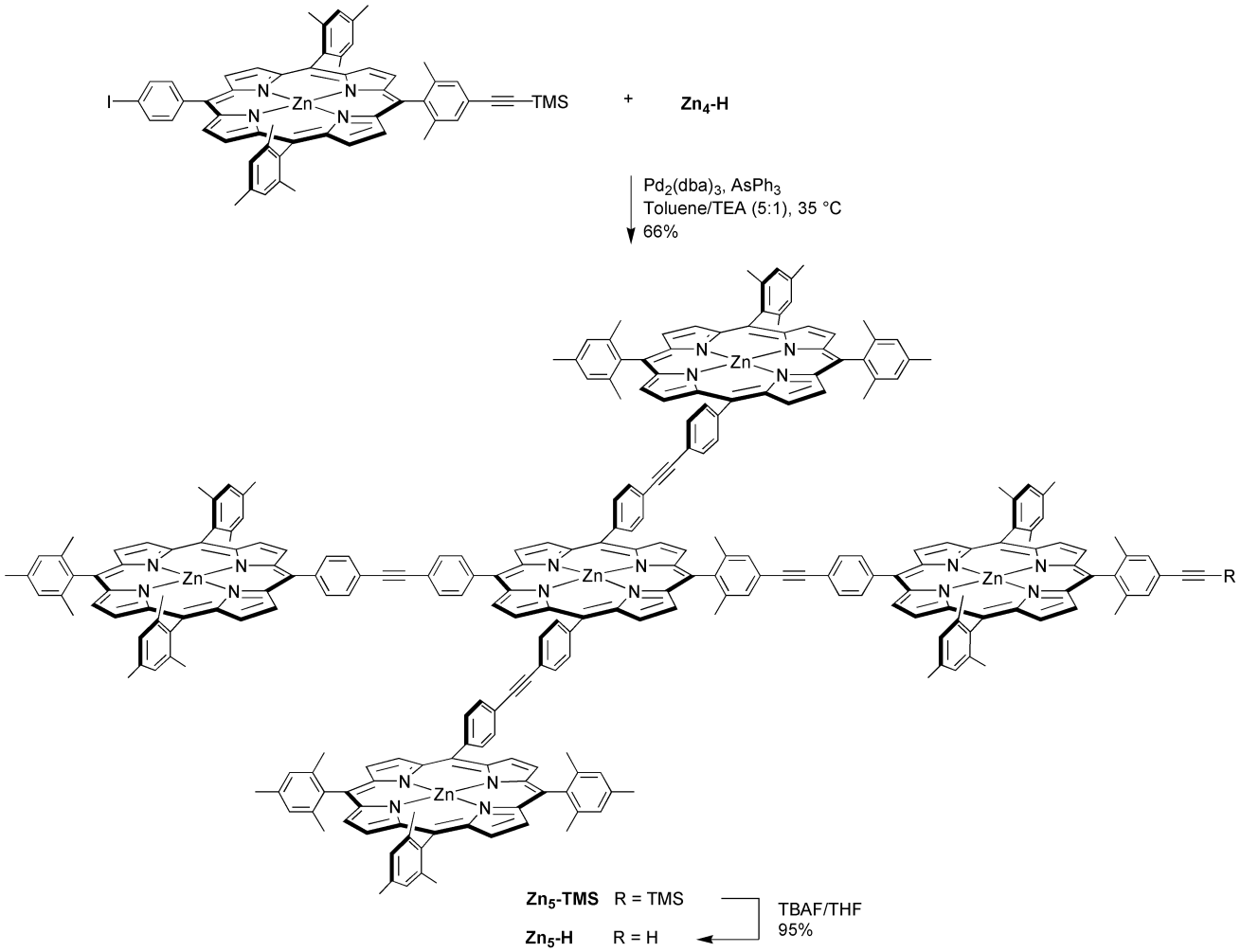

Scheme 4 Synthesis of pentameric porphyrin building blocks.[50]

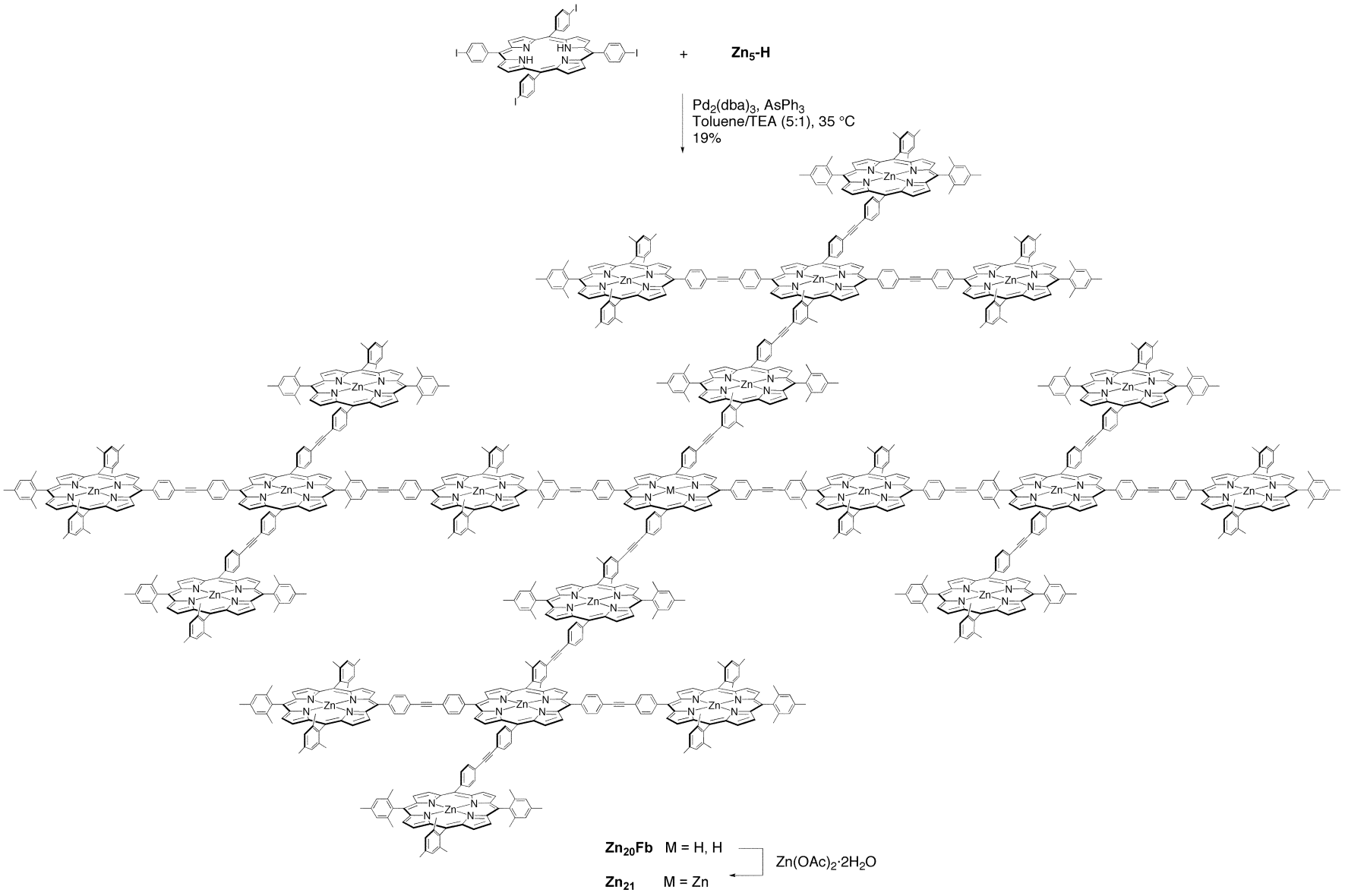

Scheme 5 Synthesis of $Zn_{20}Fb$ and Zn_{21}.[50]

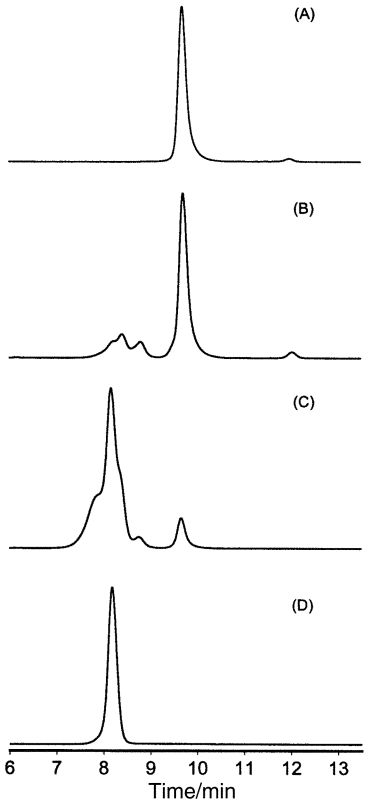

Fig. 2 SEC traces for the synthesis of $Zn_{20}Fb$ using a 10^3 Å column in series with a guard column. (A) Reaction mixture before the addition of Pd catalyst. (B) Reaction mixture after 3.5 h. (C) Reaction mixture after 22 h. (D) Purified $Zn_{20}Fb$.

Zn_9 and Zn_{21}, are essentially identical to that of the isolated ZnTPP reference compound. These spectra include the Q(0,0) emission at $\sim$595 nm and the Q(0,1) band at $\sim$650 nm (selected spectra are shown in the Electronic Supplementary Information†). These findings are in keeping with the absorption results described above, and indicate relatively weak

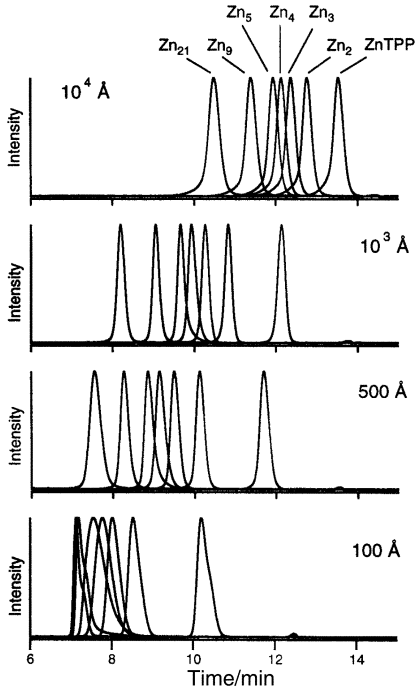

Fig. 3 Analytical SEC elution profiles of porphyrin arrays using columns of different pore sizes. The labels "Zn_4" and "Zn_5" refer to Zn_4-TMS and Zn_5-TMS, respectively.

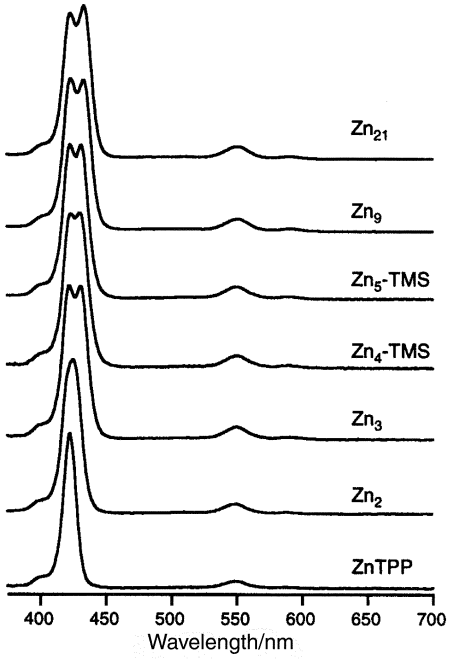

Fig. 4 Absorption spectra of Zn-porphyrin arrays in toluene at room temperature, showing the strong near-UV Soret B band(s) and the weaker visible Q bands.

perturbations of the porphyrin excited-state spectral properties in the large arrays relative to the isolated chromophores. Furthermore, the emission yields of $\Phi_f = 0.033$ for the all-Zn-porphyrin arrays Zn_9 and Zn_{21} in toluene at room temperature are found to be the same as that for the ZnTPP reference monomer ($\Phi_f = 0.033$).[59] This finding again demonstrates that the inherent excited-state decay processes in the monomer are preserved in the very large arrays, including the 21-mer, with the same microscopic rate constants as in the reference monomer. These emission-yield results also demonstrate the absence of deleterious quenching processes among the

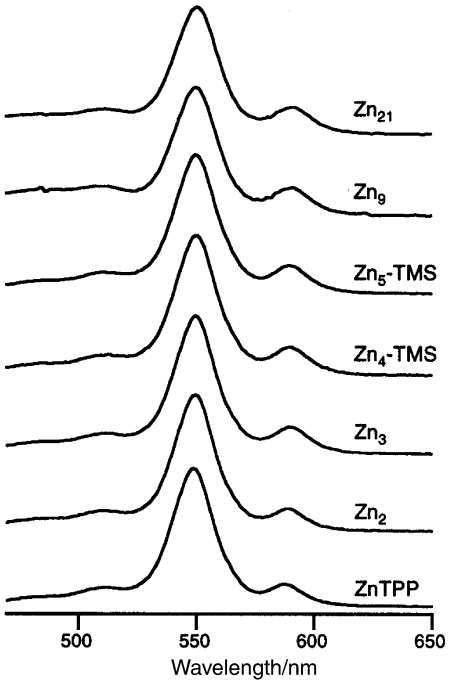

Fig. 5 Absorption spectra of the Zn-porphyrin arrays shown in Fig. 4, but focusing on the visible, Q-band region.

Table 1 UV/Vis spectral data for multiporphyrin arrays and reference monomer

	Soret (B) region				Visible (Q) region			
Compound	λ_{max}/nm	ε/M^{-1} cm^{-1} $\times 10^5$	λ_{max}/nm	ε/M^{-1} cm^{-1} $\times 10^5$	λ_{max}/nm	ε/M^{-1} cm^{-1} $\times 10^4$	λ_{max}/nm	ε/M^{-1} cm^{-1} $\times 10^4$
ZnTPP	423	5.2			549	2.2	588	0.34
Zn_2	426	6.8			550	4.3	588	0.72
Zn_3	423	8.9	431	8.9	550	6.9	590	1.4
Zn_4-TMS	424	14	431	14	550	11	591	2.2
Zn_5-TMS	423	14	432	14	550	11	590	2.2
Zn_8Fb	423	17	432	18	550	15	590	3.6
$Zn_{20}Fb$	423	49	433	52	550	42	590	8.9

Zn-porphyrins in the large arrays. If present, such quenching processes could compromise energy transfer from the Zn-porphyrin light-harvesting chromophores to the central Fb-porphyrin site in the Zn_8Fb and $Zn_{20}Fb$ arrays.

The fluorescence spectra of the Zn_8Fb and $Zn_{20}Fb$ arrays are dominated by emission from the central, single Fb-porphyrin component, even when the Zn-porphyrins are predominantly excited at 550 nm (Fig. 6, insets). These emission features are ascribable to the Fb-porphyrin $Q_X(0,0)$ and $Q_X(0,1)$ bands at $\sim$650 and $\sim$720 nm. The spectra of these large arrays also show a small amount of fluorescence from the large Zn-porphyrin pool, as is indicated by Q(0,0) Zn-porphyrin emission at $\sim$600 nm. Integration of the total emission (Zn- plus Fb-porphyrins from 565 to 800 nm) using predominant Zn-porphyrin excitation at 550 nm gives a total emission yield of 0.084 for $Zn_{20}Fb$ and 0.050 for Zn_8Fb in toluene at room temperature. These values can be compared with the emission yields of $\Phi_f = 0.033$ for ZnTPP and $\Phi_f = 0.11$ for FbTPP.[57,59] The observations that the total emission yields in the large arrays are less than that for FbTPP and that some residual Zn-porphyrin emission is observed both indicate that energy transfer to the central Fb-porphyrin is high, but not quantitative. However, it is difficult to draw quantitative conclusions of the energy-transfer efficiency from these emission studies alone (and the value for Zn_8Fb seems anomalously low; *vide infra*). This is so because of (1) the technical difficulties associated with making detailed comparisons (which arise because of the large differences in relative absorption intensities in the large arrays and reference monomers), (2) the presence of emission from two types of porphyrins in the arrays, and (3) the effect on the apparent yields of only a minor Zn-porphyrin impurity in the large assemblies. Thus, estimates for the efficiency of energy transfer from the Zn-porphyrin light-harvesting components to the central Fb-porphyrin in $Zn_{20}Fb$ and ZnF_8Fb are best made from the time-resolved absorption studies described below. These latter results are generally in good agreement with the emission data described above.

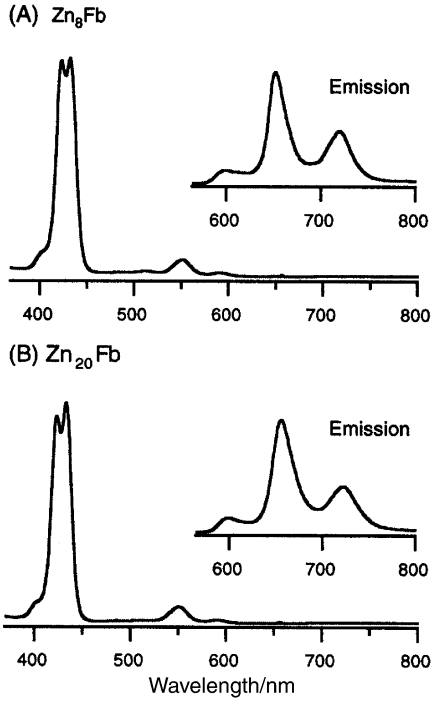

Fig. 6 Absorption spectra of Zn_8Fb and $Zn_{20}Fb$ in toluene at room temperature. The insets show emission spectra in toluene using $\lambda_{ex} = 550$ nm.

Transient absorption spectroscopy. Energy transfer from the Zn-porphyrin components of Zn_8Fb and $Zn_{20}Fb$ to the central Fb-porphyrin was investigated with time-resolved absorption spectroscopy. Predominant Zn-porphyrin excitation was achieved by using 130 fs excitation flashes at 550 nm, where the absorption of the single Fb-porphyrin is very small compared to that of the multiple Zn-porphyrins. The features in the transient difference spectra can be assigned to the excited singlet states of the Zn-porphyrin (Zn*) or the Fb-porphyrin (Fb*) based on characteristics in the static absorption and fluorescence spectra, as described previously for smaller arrays containing a Fb-porphyrin and one or more Zn-porphyrins.[15,16,19,20]

Fig. 7 shows representative absorption difference spectra for Zn_8Fb in toluene at room temperature. The spectrum at 1 ps contains the features expected for Zn*, the most prominent of which is the bleaching of the Q(1,0) ground-state absorption band at $\sim$550 nm. Other Zn* features include the Q(2,0) bleaching at 510 nm, Q(0,0) bleaching and stimulated emission

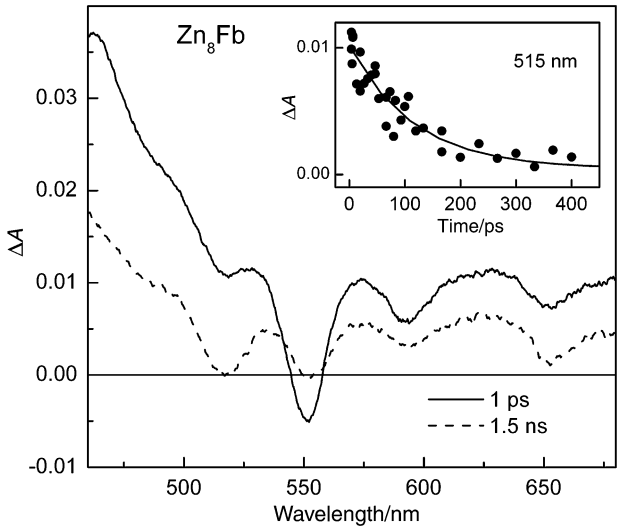

Fig. 7 Time-resolved absorption spectra for Zn_8Fb in toluene at room temperature, obtained using 130 fs excitation flashes at 550 nm. The inset shows a kinetic profile at 515 nm and a fit, giving an effective Zn* lifetime in the array of 105 ps (data before and during the flash and between 500 ps and 3.5 ns not shown for clarity).

at ~590 nm, and Q(0,1) stimulated emission at 650 nm. The Zn* features have largely decayed by 1.5 ns, and characteristics of Fb* have developed, as a result of energy funneling to the central porphyrin of the Zn_8Fb array (Scheme 3). The most notable signatures of the overall Zn*Fb→ZnFb* energy-transfer process are the decay of Zn-porphyrin bleaching at 550 nm and growth of the Fb-porphyrin $Q_Y(1,0)$ bleaching at 515 nm (along with partial decay of the broad transient absorption extending from 450 to past 700 nm). Other Fb* features include $Q_Y(0,0)$ and $Q_X(1,0)$ ground-state absorption bands at 550 and 590 nm, together with $Q_X(0,0)$ bleaching and stimulated emission at 650 nm. Some of these features have similar positions to Zn* features, but have different intensity ratios as expected from the static optical spectra. In addition to the dominant contribution of Fb* to the 1.5 ns spectrum, there also appears to be some small residual Zn* contribution that most likely arises from monomeric pigments formed by minor decomposition.

A representative time profile at 515 nm is shown in the inset to Fig. 7 (with data before and during the flash, and between 500 ps and 3.5 ns, not shown for clarity). The kinetic profiles at this and other wavelengths (*e.g.*, 460 and 550 nm) are dominated by a component having a time constant of 105 ± 15 ps, obtained by averaging values from these regions on repeated samples. As is discussed below, this value represents the effective Zn* lifetime in the array, which decays essentially quantitatively *via* transfer of energy to the Fb-component. Inclusion of an additional, smaller amplitude component having a time constant of several nanoseconds gives the best fits, and this component is consistent with the presence of a small amount of monomeric Zn* resulting from minor decomposition. The presence of this kinetic component and the minor decomposition product does not affect the interpretation of spectral and kinetic data associated with the decay of Zn* or energy flow in the arrays. It is noteworthy that a fast component having a time constant of ~10 ps is observed with increasing amplitude as the photon flux is progressively increased over that used for the measurements depicted in Fig. 7. This component is ascribed to Zn*Zn*→Zn*Zn excited-state annihilation involving multiple Zn* produced in a given array at high (but not low) excitation intensities.[60] It is also noteworthy that the dominant 105 ps component (due to overall Zn*Fb→ZnFb* energy transfer) is unchanged within experimental error as the excitation intensity is varied.

Similar transient absorption studies were performed for the larger array $Zn_{20}Fb$ in toluene at room temperature. A time constant of 220 ± 40 ps is obtained from measurements at several wavelengths (*e.g.*, 515 and 550 nm) on multiple samples using different excitation intensities. A fast component having a time constant of ~7 ps is found at high, but not low, excitation intensities.

For comparison, the time constant for decay of the Zn bleaching and formation of the Fb bleaching for the ZnZnFb triad (Chart 2) is 90 ± 10 ps in toluene at room temperature (average of values in the two regions obtained here and previously[20]); this triad exhibits a fast component with a time constant of ~3 ps at high excitation intensities. For the simpler ZnFbP dyad (Chart 1), the kinetic profiles in both the Zn- and Fb-porphyrin bleaching regions give a time constant of 45 ± 4 ps (average of values found here and previously[20]); the dyad shows no shorter-lived component at high excitation intensities because excitation of two Zn-porphyrins and consequent excited-state annihilation is not possible in this case. ZnFbP has the same methyl-group steric hindrance on the diarylethyne linker that is present between the Fb-porphyrin core and the adjacent Zn-porphyrins in Zn_8Fb and $Zn_{20}Fb$ (Schemes 3 and 5). The related dyad ZnFbU, which has an unhindered linker,[61] exhibits a shorter time constant of 24 ± 2 ps.[20]

The dominant time constant represents the average Zn* lifetime in each of the arrays; this time constant is independent of excitation intensity. When compared with the much longer ~2.4 ns Zn* lifetime of monomeric Zn-porphyrins, it is also seen that these values are the same within error as the calculated average time constant for energy to arrive from the Zn-porphyrin pool to the Fb-porphyrin core.[62] For each array, the energy-transfer time constant represents an average value that includes a range of overall transfer times to the core unit depending on which Zn-porphyrin is initially excited. In particular, the time depends on the distance of the initially excited Zn* to the core and thus, the number of transfer steps between Zn-porphyrins (which includes reversible back-and-forth transfers) before the final irreversible transfer to the central Fb-porphyrin. The data described above show that this overall transfer time to the core unit increases with increasing size of the array in the following order: ZnFbP (45 ps) < ZnZnFb (90 ps) < Zn_8Fb (105 ps) < $Zn_{20}Fb$ (220 ps). Following established analyses,[19,20,44,53] the lifetimes can be used to obtain (average) yields of energy transfer from the Zn-porphyrin(s) to the central Fb-porphyrin *via* the formula $\Phi_{trans} = 1 - \tau_A/\tau_M$, where τ_A is the time constant measured in the array and $\tau_M = 2.4$ ns for the reference monomer. Thus, the overall energy-transfer efficiencies are ZnFbP (98%) < ZnZnFb (96%) < Zn_8Fb (96%) < $Zn_{20}Fb$ (92%). The latter value is in reasonable agreement with the fluorescence quantum yield measured for this compound.

The trends and relative values of the overall transfer times for energy trapping at the core porphyrin are consistent with the structures of the various arrays. In particular, the minimal number of transfer steps between Zn-porphyrins (ignoring reversible back-and-forth hops) on a path directly to the central Fb-porphyrin will be, depending on which Zn-porphyrin is excited, as follows: either 2, 1, or zero for $Zn_{20}Fb$; either 1 or 0 for Zn_8Fb; either 1or 0 for ZnZnFb; and 0 for ZnFbP. Thus, it is reasonable that the smallest increment in transfer time between members of this series occurs between ZnZnFb (105 ps; Chart 2) and Zn_8Fb (90 ps; Scheme 3); in both arrays the most peripheral Zn-porphyrin is only one Zn-porphyrin removed from the central Fb-porphyrin. The modestly longer arrival time at the core for Zn_8Fb *versus* ZnZnFb can be explained in terms of the different topologies of the two arrays. In particular, for Zn_8Fb more reversible transfers (hops) between Zn-porphyrins are possible owing to the branched architecture in each of the two Zn_4 arms.

The above arguments also imply that the overall transfer time for $Zn_{20}Fb$ should be the longest among the arrays, as is observed. For this large array, energy-transfer processes can originate in the four most peripheral Zn-porphyrins, which are much farther from the Fb-porphyrin than are the two most peripheral Zn-porphyrins in Zn_8Fb. Hence, more back-and-forth transfers can occur between Zn-porphyrins in $Zn_{20}Fb$. Likewise, the fastest transfer times are expected for the ZnFbP (and ZnFbU) dyad because the sole Zn-porphyrin excited-state donor has no choice but to transfer energy to the adjacent Fb-porphyrin acceptor.

One of the primary objectives in preparing progressively larger arrays was to increase the light-harvesting ability of the architectures. The new Zn_8Fb and $Zn_{20}Fb$ structures have achieved this goal. The enhanced light-harvesting ability with increasing size of the array is clearly reflected in the static optical spectra, which show the dramatically increasing extinction of the overlapping $S_0 \rightarrow S_1$ absorption bands of the Zn-porphyrin light-harvesting chromophores relative to the single Fb-porphyrin energy trap. The light-harvesting ability of the arrays is also reflected in the static emission and time-resolved absorption characteristics, which reveal rapid energy transfer to the central unit. It is interesting to note that in going from the ZnZnFb triad to the Zn_8Fb nonamer, there is a four-fold increase in the light-gathering ability (due to the increased number of Zn-porphyrins), but the average overall time for arrival of energy at the Fb-porphyrin core increases only

modestly (from 90 to 105 ps). Again, these factors can be rationalized in terms of the structures of the triad and nonamer. However, more detailed considerations of the photodynamics in these two arrays (and $Zn_{20}Fb$) must also take into account the fact that significant electronic communication between nonadjacent porphyrins can occur *via* a superexchange mediated process involving an intervening porphyrin.[21] The communication between distant sites is expected to enhance the rates and efficiencies of energy transfer from the pool of light-harvesting pigments to the central porphyrin core.

7. Electrochemistry

We have previously investigated the electrochemical characteristics of dimeric (Zn_2, ZnFbU, ZnFbP),[4] trimeric (Zn_3, ZnZnFb),[4] and star-shaped pentameric (Zn_4FbU,[19] Zn_5U,[19] and others[3]) multiporphyrin arrays (Charts 1 and 2). Earlier bulk electrolysis studies of the star-shaped pentameric arrays showed that as many as eight electrons could be removed from the array to yield a stable, highly oxidized π-cation radical.[3,19] Removal of additional electrons results in decomposition of the array. The fact that a large number of oxidizing equivalents can potentially be stored in multiporphyrin arrays prompted us to investigate hole storage in the largest array described herein, the 21-mer $Zn_{20}Fb$.

The voltammetric characteristics of $Zn_{20}Fb$ are similar to those we have measured for other multiporphyrin arrays.[3,4,19] In particular, the 21-mer exhibits two reversible oxidation waves ($E_{1/2}(1)$ ~0.5 V; $E_{1/2}(2)$ ~0.9 V; *versus* Ag/Ag^+ in benzonitrile at room temperature; Fc/Fc^+, $E_{1/2}=0.11$ V). These waves correspond to the first and second oxidations of the porphyrin ring. The $E_{1/2}$ values for the 20 weakly interacting Zn-porphyrins are very similar and cannot be resolved. In principle, the oxidation waves for the Fb-porphyrin should be resolvable (because the $E_{1/2}$ values for this component are higher than those of the Zn- porphyrins[3]); however, the waves for the single Fb-porphyrin are completely masked by the waves from the large number of Zn-porphyrins. The redox potentials observed for the porphyrins in the 21-mer are essentially the same as those found previously in star-shaped pentameric and smaller arrays and in the isolated chromophores. This observation is indicative of relatively weak ground-state interactions between the constituent porphyrins in the 21-mer, as has been found previously for smaller arrays.[3,4,19]

Bulk electrolysis studies were carried out on $Zn_{20}Fb$ to investigate the hole-storage capabilities of this array. The progress of the bulk oxidation was monitored optically as shown in Fig. 8 which depicts the 500–1000 nm region of the absorption spectrum (the region in which porphyrin π-cation radicals exhibit the most characteristic spectral features[3]). As more electron equivalents are removed from the array, the broad, near-infrared optical signatures of a porphyrin π-cation become more pronounced. When 21 electron equivalents have been removed, the Q-band features characteristic of the neutral porphyrin have completely disappeared and only features of a porphyrin π-cation radical remain. These spectral characteristics indicate that the equivalent of one hole resides on each of the 21 porphyrins in the array. The $(Zn_{20}Fb)^{21+}$ species was relatively stable and exhibited no evidence of decomposition. The bulk-oxidized array was subsequently reduced with the recovery of ⩾95% of the neutral material. The "supercharged" cation was also quite soluble and showed no evidence of precipitation. Attempts were not made to remove additional electrons from the array; however, the stability of $(Zn_{20}Fb)^{21+}$, along with our previous observation that up to eight holes can be stored in star-shaped pentameric arrays (Zn_4FbU, Zn_5U, others),[3,19] suggest that even more holes could be reversibly stored in the 21-mer.

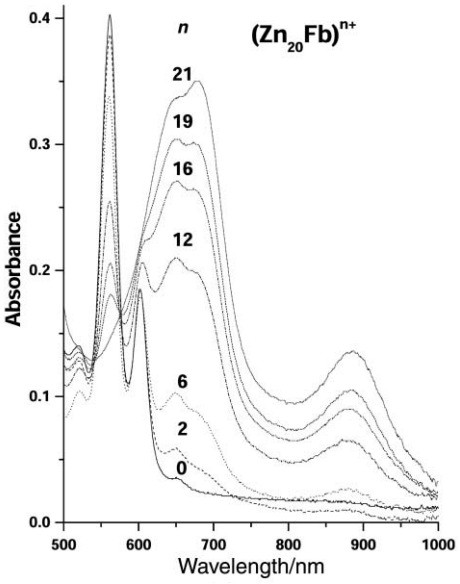

Fig. 8 Spectroelectrochemistry of $(Zn_{20}Fb)^{n+}$ in benzonitrile ($n=0$, 2, 6, 12, 16, 19, and 21). The number on each spectrum represents the value of n.

8 Conclusion

A convergent building block synthesis has been used to prepare a number of dendrimeric diarylethyne-linked porphyrin arrays, with the largest containing 21 chromophores. The light-harvesting ability of the arrays increases with the size of the array due to the increasing optical absorption cross-section afforded by the multiple Zn-porphyrins. The Zn-porphyrins funnel the excited-state electronic energy to the Fb-porphyrin at the core of the array. These same multiporphyrin arrays also serve as effective ground-state hole storage reservoirs, in that at least one electron can be removed from each chromophore in the assembly. The covalent diarylethyne linkages provide significant electronic communication between the chromophores but do not compromise characteristics that can be designed into building blocks, such as redox potentials and inherent photophysical properties of the lowest excited singlet state. Thus, this strategy complements approaches in which much stronger coupling between the units significantly modulates the properties of the units with increasing size and complexity of the overall array. From a synthetic standpoint, this building block approach enables facile synthesis of modestly sized arrays but the isolation of larger arrays in pure form requires extensive chromatography. The limitations encountered by the use of repetitive Pd-coupling reactions in this domain caused us (1) to develop refined conditions for Pd-coupling reactions with porphyrins,[48] (2) to develop synthetic strategies that employ sequences of complementary chemistries in the construction of arrays,[17,44] and (3) to investigate the use of non-covalent self-assembly of monomers and small covalently linked arrays to form the desired architecture.[63] The good solubility, light-harvesting, and hole-storage properties of the dendrimeric arrays described herein, in conjunction with these new synthetic approaches, augurs well for the design and synthesis of larger multiporphyrin arrays of interest for a variety of applications.

Acknowledgement

This research was supported by a grant from the Division of Chemical Sciences, Office of Basic Energy Sciences, Office of Energy Research, U. S. Department of Energy (to J. S. L.), and grants from the NIH (GM 36485 to D. H.; GM 39781 to D. F. B.). Mass spectra were obtained at the Mass Spectrometry Laboratory for Biotechnology at North Carolina State University. Partial funding for the Facility was obtained from

the North Carolina Biotechnology Center and the NSF. We thank Dr. Robert Donohoe for helpful discussions, Dr. Dongho Kim for assisting with some of the transient absorption measurements, and Prof. David C. Mauzerall for exploratory studies of multiphoton effects in the all-Zn-arrays.

References

1 A portion of this work was adapted from the Ph.D. thesis of Thomas E. Johnson, Department of Chemistry, Carnegie Mellon University, 1995.
2 R. W. Wagner, T. E. Johnson and J. S. Lindsey, *J. Am. Chem. Soc.*, 1996, **118**, 11166.
3 J. Seth, V. Palaniappan, T. E. Johnson, S. Prathapan, J. S. Lindsey and D. F. Bocian, *J. Am. Chem. Soc.*, 1994, **116**, 10578.
4 J. Seth, V. Palaniappan, R. W. Wagner, T. E. Johnson, J. S. Lindsey and D. F. Bocian, *J. Am. Chem. Soc.*, 1996, **118**, 11194.
5 (*a*) D. P. Arnold, A. W. Johnson and M. Mahendran, *J. Chem. Soc., Perkin Trans. 1*, 1978, 366; (*b*) D. P. Arnold and L. J. Nitschinsk, *Tetrahedron*, 1992, **48**, 8781; (*c*) D. P. Arnold and L. J. Nitschinsk, *Tetrahedron Lett.*, 1993, **34**, 693; (*d*) D. P. Arnold, D. A. James, C. H. L. Kennard and G. Smith, *J. Chem. Soc., Chem. Commun.*, 1994, 2131.
6 (*a*) S. Anderson, S. J. Martin and D. D. C. Bradley, *Angew. Chem., Int. Ed. Engl.*, 1994, **33**, 655; (*b*) H. L. Anderson, *Inorg. Chem.*, 1994, **33**, 972.
7 J. J. Gosper and M. Ali, *J. Chem. Soc., Chem. Commun.*, 1994, 1707.
8 (*a*) V. S.-Y. Lin, S. G. DiMagno and M. J. Therien, *Science*, 1994, **264**, 1105; (*b*) V. S.-Y. Lin and M. J. Therien, *Chem. Eur. J.*, 1995, **1**, 645.
9 (*a*) K. Susumu, T. Shimidzu, K. Tanaka and H. Segawa, *Tetrahedron Lett.*, 1996, **46**, 8399; (*b*) A. Osuka and H. Shimidzu, *Angew. Chem., Int. Ed. Engl.*, 1997, **36**, 135; (*c*) N. Yoshida, H. Shimidzu and A. Osuka, *Chem. Lett.*, 1998, 55; (*d*) T. Ogawa, Y. Nishimoto, N. Yoshida, N. Ono and A. Osuka, *Chem. Commun.*, 1998, 337; (*e*) A. Nakano, A. Osuka, I. Yamazaki, T. Yamazaki and Y. Nishimura, *Angew. Chem., Int. Ed.*, 1998, **37**, 3023; (*f*) T. Ogawa, Y. Nishimoto, N. Yoshida, N. Ono and A. Osuka, *Angew. Chem., Int. Ed.*, 1999, **38**, 176; (*g*) N. Yoshida, N. Aratani and A. Osuka, *Chem. Commun.*, 2000, 197; (*h*) N. Aratani, A. Osuka, Y. H. Kim, D. H. Jeong and D. Kim, *Angew. Chem., Int. Ed.*, 2000, **39**, 1458.
10 (*a*) C. Devadoss, P. Bharathi and J. S. Moore, *J. Am. Chem. Soc.*, 1996, **118**, 9635; (*b*) S. F. Swallen, R. Kopelman, J. S. Moore and C. Devadoss, *J. Mol. Struct.*, 1999, **485–486**, 585; (*c*) S. F. Swallen, Z.-Y. Shi, W. Tan, Z. Xu, J. S. Moore and R. Kopelman, *J. Lumin.*, 1998, **76–77**, 193; (*d*) Y. Wakabayashi, M. Tokeshi, D.-L. Jiang, T. Aida and T. Kitamori, *J. Lumin.*, 1999, **83–84**, 313.
11 M. A. Miller, R. K. Lammi, S. Prathapan, D. Holten and J. S. Lindsey, *J. Org. Chem.*, 2000, **65**, 6634.
12 S. Prathapan, T. E. Johnson and J. S. Lindsey, *J. Am. Chem. Soc.*, 1993, **115**, 7519.
13 R. W. Wagner and J. S. Lindsey, *J. Am. Chem. Soc.*, 1994, **116**, 9759.
14 R. W. Wagner, J. S. Lindsey, J. Seth, V. Palaniappan and D. F. Bocian, *J. Am. Chem. Soc.*, 1996, **118**, 3996.
15 R. W. Wagner, J. Seth, S. I. Yang, D. Kim, D. F. Bocian, D. Holten and J. S. Lindsey, *J. Org. Chem.*, 1998, **63**, 5042.
16 J. Li, A. Ambroise, S. I. Yang, J. R. Diers, J. Seth, C. R. Wack, D. F. Bocian, D. Holten and J. S. Lindsey, *J. Am. Chem. Soc.*, 1999, **121**, 8927.
17 J. Li and J. S. Lindsey, *J. Org. Chem.*, 1999, **64**, 9101.
18 (*a*) D. Kuciauskas, P. A. Liddell, T. E. Johnson, S. J. Weghorn, J. S. Lindsey, A. L. Moore, T. A. Moore and D. Gust, *J. Am. Chem. Soc.*, 1999, **121**, 8604; (*b*) G. Kodis, P. A. Liddell, L. de la Garza, P. C. Clausen, J. S. Lindsey, A. L. Moore, T. A. Moore and D. Gust, *J. Phys. Chem. B*, in press.
19 F. Li, S. Gentemann, W. A. Kalsbeck, J. Seth, J. S. Lindsey, D. Holten and D. F. Bocian, *J. Mater. Chem.*, 1997, **7**, 1245.
20 J.-S. Hsiao, B. P. Krueger, R. W. Wagner, T. E. Johnson, J. K. Delaney, D. C. Mauzerall, G. R. Fleming, J. S. Lindsey, D. F. Bocian and R. J. Donohoe, *J. Am. Chem. Soc.*, 1996, **118**, 11181.
21 R. K. Lammi, A. Ambroise, T. Balasubramanian, R. W. Wagner, D. F. Bocian, D. Holten and J. S. Lindsey, *J. Am. Chem. Soc.*, 2000, **122**, 7579.
22 N. Nishino, R. W. Wagner and J. S. Lindsey, *J. Org. Chem.*, 1996, **61**, 7534.
23 J. S. Lindsey, S. Prathapan, T. E. Johnson and R. W. Wagner, *Tetrahedron*, 1994, **50**, 8941.
24 C. M. Drain, F. Nifiatis, A. Vasenko and J. D. Batteas, *Angew. Chem., Int. Ed.*, 1998, **37**, 2344.
25 H. Tamiaki, T. Miyatake, R. Tanikaga, A. R. Holzwarth and K. Schaffner, *Angew. Chem., Int. Ed. Engl.*, 1996, **35**, 772.
26 R. A. Haycock, A. Yartsev, U. Michelsen, V. Sundström and C. A. Hunter, *Angew. Chem., Int. Ed.*, 2000, **39**, 3616.
27 (*a*) J.-C. Chambron, V. Heitz and J.-P. Sauvage, in *The Porphyrin Handbook*, eds. K. M. Kadish, K. M. Smith and R. Guilard, Academic Press, San Diego, CA, 2000, vol. 6, pp. 1–42; (*b*) J. Wojaczynski and L. Latos-Grazynski, *Coord. Chem. Rev.*, 2000, **204**, 113; (*c*) T. Imamura and K. Fukushima, *Coord. Chem. Rev.*, 2000, **198**, 133.
28 (*a*) B. Wang, S.-W. Yang and W. E. Jones Jr, *Chem. Mater.*, 1997, **9**, 2031; (*b*) B. Jiang, S.-W. Yang, R. Niver and W. E. Jones Jr, *Synth. Met.*, 1998, **94**, 205.
29 B. Jiang, S.-W. Yang, D. C. Barbini and W. E. Jones Jr, *Chem. Commun.*, 1998, 213.
30 P. N. Taylor, J. Huuskonen, G. Rumbles, R. T. Aplin, E. Williams and H. L. Anderson, *Chem. Commun.*, 1998, 909.
31 (*a*) A. K. Burrell and D. L. Officer, *SYNLETT*, 1998, 1297; (*b*) D. L. Officer, A. K. Burrell and D. C. W. Reid, *Chem. Commun.*, 1996, 1657.
32 (*a*) O. Mongin, C. Papamicaël, N. Hoyler and A. Gossauer, *J. Org. Chem.*, 1998, **63**, 5568; (*b*) O. Mongin and A. Gossauer, *Tetrahedron*, 1997, **53**, 6835; (*c*) O. Mongin, N. Hoyler and A. Gossauer, *Eur. J. Org. Chem.*, 2000, 1193; (*d*) O. Mongin, A. Schuwey, M.-A. Vallot and A. Gossauer, *Tetrahedron Lett.*, 1999, **40**, 8347.
33 J. Wytko, V. Berl, M. McLaughlin, R. R. Tykwinski, M. Schreiber, F. Diederich, C. Boudon, J.-P. Gisselbrecht and M. Gross, *Helv. Chim. Acta*, 1998, **81**, 1964.
34 (*a*) S. Anderson, H. L. Anderson, A. Bashall, M. McPartlin and J. K. M. Sanders, *Angew. Chem., Int. Ed. Engl.*, 1995, **34**, 1096; (*b*) J. K. M. Sanders, in *The Porphyrin Handbook*, eds. K. M. Kadish, K. M. Smith and R. Guilard, Academic Press, San Diego, CA, 2000, vol. 3, pp. 347–368.
35 (*a*) H. Higuchi, M. Takeuchi and J. Ojima, *Chem. Lett.*, 1996, 593; (*b*) R. Gauler and N. Risch, *Tetrahedron Lett.*, 1997, **38**, 223; (*c*) R. Gauler and N. Risch, *Eur. J. Org. Chem.*, 1998, 1193.
36 (*a*) O. Wennerström, H. Ericsson, I. Raston, S. Svensson and W. Pimlott, *Tetrahedron Lett.*, 1989, **30**, 1129; (*b*) D. Hammel, P. Erk, B. Schuler, J. Heinze and K. Mullen, *Adv. Mater.*, 1992, **4**, 737; (*c*) A. Osuka, B.-L. Liu and K. Maruyama, *Chem. Lett.*, 1993, 949; (*d*) A. Osuka, N. Tanabe, S. Nakajima and K. Maruyama, *J. Chem. Soc., Perkin Trans. 2*, 1996, 199.
37 K. Sugiura, H. Tanaka, T. Matsumoto, T. Kawai and Y. Sakata, *Chem. Lett.*, 1999, 1193.
38 T. Norsten and N. Branda, *Chem. Commun.*, 1998, 1257.
39 S. Hecht, T. Emrick and J. M. Fréchet, *Chem. Commun.*, 2000, 313.
40 K. Ichihara and Y. Naruta, *Chem. Lett.*, 1995, 631.
41 E. K. L. Yeow, K. P. Ghiggino, J. N. H. Reek, M. J. Crossley, A. W. Bosman, A. P. H. J. Schenning and E. W. Meijer, *J. Phys. Chem. B*, 2000, **104**, 2596.
42 (*a*) N. Maruo, M. Uchiyama, T. Kato, T. Arai, H. Akisada and N. Nishino, *Chem. Commun.*, 1999, 2057; (*b*) T. Kato, M. Uchiyama, N. Maruo, T. Arai and N. Nishino, *Chem. Lett.*, 2000, 144.
43 (*a*) C. C. Mak, N. Bampos and J. K. M. Sanders, *Chem. Commun.*, 1999, 1085; (*b*) C. C. Mak, N. Bampos and J. K. M. Sanders, *Angew. Chem., Int. Ed.*, 1998, **37**, 3020.
44 J. Li, J. R. Diers, J. Seth, S. I. Yang, D. F. Bocian, D. Holten and J. S. Lindsey, *J. Org. Chem.*, 1999, **64**, 9090.
45 D.-L. Jiang and T. Aida, *J. Am. Chem. Soc.*, 1998, **120**, 10895.
46 (*a*) K. Sonogashira, Y. Tohda and N. Hagihara, *Tetrahedron Lett.*, 1975, 4467; (*b*) H. A. Dieck and F. R. Heck, *J. Organomet. Chem.*, 1975, **93**, 259; (*c*) L. Cassar, *J. Organomet. Chem.*, 1975, **93**, 253.
47 R. W. Wagner, T. E. Johnson, F. Li and J. S. Lindsey, *J. Org. Chem.*, 1995, **60**, 5266.
48 R. W. Wagner, Y. Ciringh, P. C. Clausen and J. S. Lindsey, *Chem. Mater.*, 1999, **11**, 2974.
49 A. A. Bothner-By, J. Dadok, T. E. Johnson and J. S. Lindsey, *J. Phys. Chem.*, 1996, **100**, 17551.
50 The arrays are displayed for clarity with coplanar porphyrins in a 2-dimensional sheet-like conformation. However, free rotation about the ethyne and bending about the diphenylethyne linker[49]

enable a range of 3-dimensional conformations of the multi-porphyrin arrays.
51 A. Ambroise, R. W. Wagner, P. D. Rao, J. A. Riggs, P. Hascoat, J. R. Diers, J. Seth, R. K. Lammi, D. F. Bocian, D. Holten and J. S. Lindsey, *Chem. Mater.*, 2001, **13**, 1023.
52 The nomenclature for the dimers included a designation to identify the type of linker (U = unhindered; P = proximal hindered) joining the porphyrins. This linker terminology has not been included in the large arrays described herein.
53 (*a*) J. P. Strachan, S. Gentemann, J. Seth, W. A. Kalsbeck, J. S. Lindsey, D. Holten and D. F. Bocian, *J. Am. Chem. Soc.*, 1997, **119**, 11191; (*b*) J. P. Strachan, S. Gentemann, J. Seth, W. A. Kalsbeck, J. S. Lindsey, D. Holten and D. F. Bocian, *Inorg. Chem.*, 1998, **37**, 1191; (*c*) S. I. Yang, J. Seth, T. Balasubramanian, D. Kim, J. S. Lindsey, D. Holten and D. F. Bocian, *J. Am. Chem. Soc.*, 1999, **121**, 4008.
54 C.-H. Lee and J. S. Lindsey, *Tetrahedron*, 1994, **50**, 11427.
55 N. Srinivasan, C. A. Haney, J. S. Lindsey, W. Zhang and B. T. Chait, *J. Porphyrins Phthalocyanines*, 1999, **3**, 283.
56 D. Fenyo, B. T. Chait, T. E. Johnson and J. S. Lindsey, *J. Porphyrins Phthalocyanines*, 1997, **1**, 93.
57 M. Gouterman, in *The Porphyrins*, ed. D. Dolphin, Academic Press, New York, 1978, vol. III, pp. 1–153.
58 M. Gouterman, D. Holten and E. Lieberman, *Chem. Phys.*, 1977, **25**, 139.
59 P. G. Seybold and M. Gouterman, *J. Mol. Spectrosc.*, 1969, **31**, 1.
60 With increasing number of light-harvesting units in an array (*i.e.*, the number of Zn-porphyrins in our arrays) and/or increasing photon flux, there is the increasing possibility that more than one pigment may be excited simultaneously in a given array. The production of multiple excitations in a given array will have both spectral and kinetic consequences; such effects are observed for the Zn_8Fb and $Zn_{20}Fb$ arrays at high but not at low excitation intensities. Even when present, these effects do not significantly impact the time constant determined for arrival of energy from the Zn pool to the Fb core, and may give an indication of the time scale for energy transfer between adjacent Zn-porphyrins in the arrays (See Electronic Supplementary Information†). The consequences of multiphoton effects on photophysical behavior are well known and have been explored extensively in photosynthetic antenna systems (*Cf.* D. Mauzerall, *J. Phys. Chem.*, 1976, **80**, 2306).
61 The steric hindrance on the linker in ZnFbP (or analogous hindrance placed on the porphyrin) slows energy transfer relative to the unhindered linker in ZnFbU due to orbital overlap considerations.[19,20,53] Likewise, the rate constants for energy hopping between Zn-porphyrins in the arrays will depend on the steric hindrance in the linker.
62 Each of the measured time constants is rigorously the average Zn* lifetime of the Zn-porphyrin pool in the given array, which is ultimately dominated by energy transfer to the Fb core; this can be seen by comparison of each measured Zn* lifetime in an array (τ_A) with the Zn* lifetime of $\tau_M = 2.4$ ns for the reference monomer. Following established analyses,[19,20,44,53] the (average) transfer time from the Zn pool to the Fb core can be calculated using the expression $\tau_{trans} = [(1/(\tau_A)) - (1/(\tau_M))]$. (This equation assumes that the inherent rate constants for Zn* decay in the arrays are the same as in the isolated chromophore, which is a good approximation given the weak interporphyrin couplings and effects on the properties of the chromophores.) For $Zn_{20}Fb$, the average energy-transfer time is $\tau_{trans} = [(1/220\ ps) - (1/2.4\ ns)] = 240$ ps, which is the same value within experimental error as the measured time constant of 220 ± 40 ps. The difference between the calculated transfer time and measured average Zn* lifetime decreases with decreasing lifetime and array size. Given these points, and the fact that the measured times already reflect average properties depending on which Zn-porphyrin is excited, we use the measured time constant as a good approximation of the average transfer time from the Zn-porphyrin pool to the Fb-porphyrin core in each array.
63 A. Ambroise, J. Li, L. Yu and J. S. Lindsey, *Org. Lett.*, 2000, **2**, 2563.